

Alterations in gene expression and sensitivity to genotoxic stress following HdmX or Hdm2 knockdown in human tumor cells harboring wild-type p53

Katherine Heminger¹, Michael Markey, Meldrick Mpagi, and Steven J. Berberich

Wright State University Boonshoft School of Medicine Biochemistry & Molecular Biology Department, Dayton, OH 45435, USA

¹ current address: Procter and Gamble Co., Cincinnati OH 45241, USA

Running title: HdmX/2 loss inhibits tumor cell proliferation

Key words: p53, HdmX, Hdm2, RNAi, gene expression profiling

Correspondence: Steven J. Berberich, PhD, Wright State University Boonshoft School of Medicine Biochemistry & Molecular Biology Department, 3640 Colonel Glenn Hwy., Dayton, OH 45435

Received: 11/18/08; **accepted:** 01/03/09; **published on line:** 01/07/09

E-mail: steven.berberich@wright.edu

Copyright: © 2009 Heminger et al. This is an open-access article distributed under the terms of the Creative Commons Attribution License, which permits unrestricted use, distribution, and reproduction in any medium, provided the original author and source are credited

Abstract: While half of all human tumors possess p53 mutations, inactivation of wild-type p53 can also occur through a variety of mechanisms that do not involve p53 gene mutation or deletion. Our laboratory has been interested in tumor cells possessing wild-type p53 protein and elevated levels of HdmX and/or Hdm2, two critical negative regulators of p53 function. In this study we utilized RNAi to knockdown HdmX or Hdm2 in MCF7 human breast cancer cells, which harbor wild-type p53 and elevated levels of HdmX and Hdm2 then examined gene expression changes and effects on cell growth. Cell cycle and growth assays confirmed that the loss of either HdmX or Hdm2 led to a significant growth inhibition and G1 cell cycle arrest. Although the removal of overexpressed HdmX/2 appears limited to an anti-proliferative effect in MCF7 cells, the loss of HdmX and/or Hdm2 enhanced cytotoxicity in these same cells exposed to DNA damage. Through the use of Affymetrix GeneChips and subsequent RT-qPCR validations, we uncovered a subset of anti-proliferative p53 target genes activated upon HdmX/2 knockdown. Interestingly, a second set of genes, normally transactivated by E2F1 as cells transverse the G1-S phase boundary, were found repressed in a p21-dependent manner following HdmX/2 knockdown. Taken together, these results provide novel insights into the reactivation of p53 in cells overexpressing HdmX and Hdm2.

INTRODUCTION

Only half of all human tumors contain mutations in the p53 tumor suppressor gene [1], with the other half retaining wild-type p53 but possessing defects in the expression of p53 regulatory proteins and pathways. Under non-stress conditions, p53 protein is maintained at a low basal level by constant ubiquitination and proteasomal degradation [2]. Upon DNA damage or various types of cellular stress, p53 is stabilized and functions as a transcription factor to induce genes involved in cell cycle arrest, apoptosis, and DNA repair [3]. The stringent regulation of p53 involves a complex

network of proteins, and is critical for maintaining genomic stability and suppressing tumor formation.

Hdm2 and its structural homologue HdmX represent two essential negative regulators of p53 as demonstrated by their embryonic lethality in knockout mice and subsequent rescue by concurrent elimination of p53 [4]. Hdm2 inactivates p53 function through direct association resulting in an inhibition of transactivation [5] and, through its E3 ligase activity targeting p53, by ubiquitin-mediated proteasome degradation [6, 7]. While HdmX shows conservation in the Hdm2 E3 ligase ring finger domain through which it

can heterodimerize with Hdm2 [8, 9], HdmX lacks the ability to ubiquitinate p53 in vivo [10, 11] and thus can only antagonize p53 transactivation [12]. The heterodimerization of Hdm2 and HdmX also plays a critical role in the response to DNA damage enabling Hdm2 to promote the ubiquitination and rapid proteasomal degradation of HdmX, thereby facilitating the tumor suppressor activity of p53 [13-15]. Thus, the interactions between p53, Hdm2 and HdmX are critical for complete regulation of p53 [4].

The overexpression of either Hdm2 or HdmX can inhibit the activity of p53 and directly contribute to tumor formation. It is not surprising that either one or both proteins are found overexpressed in many human tumors and tumor cell lines which harbor wild-type p53 [16]. Diverse approaches to activate the wild-type p53 in these tumors include the use of small molecule antagonists like Nutlin to inhibit the Hdm2-p53 interaction [17-19], and the use of antisense oligonucleotides, antibodies, and small interfering RNAs directed at Hdm2 or HdmX [20-23]. Recent findings suggest that Hdm2 and HdmX are specific independent therapeutic targets for activating wild-type p53 and that anti-cancer approaches that target both Hdm2 and HdmX should be considered as a means of treatment for tumors [16, 18, 24].

This study undertook an examination of gene expression alterations and the biological effects resulting from RNAi silencing of HdmX and Hdm2 in a breast cancer cell line overexpressing both proteins. Unlike previous studies examining only the biological effect of either HdmX or Hdm2 loss, this study focuses on a cell line where both proteins are overexpressed and further complements those previous studies with a systematic examination of gene expression changes following loss of HdmX or Hdm2. Interestingly, only p53 target genes primarily associated with cell cycle arrest were induced. More striking was the repression of a large group of E2F-regulated genes upon HdmX/2 knockdown. Using siRNA approaches targeting p21, we were able to show that these E2F-regulated genes were repressed through p53 activation of p21. Furthermore, cell proliferation and colony formation assays confirmed that loss of HdmX or Hdm2 inhibited tumor cell growth and could sensitize these cells to treatment with doxorubicin. Taken together, these results suggest that in cells where both Hdm2 and HdmX are overexpressed, removal of one leads to an anti-proliferative effect in tumor cells harboring wild-type p53 and induction of p53 cell cycle arrest genes that negatively feedback onto the E2F pathway.

RESULTS

RNAi knockdown of Hdm2 and HdmX in MCF7 cells

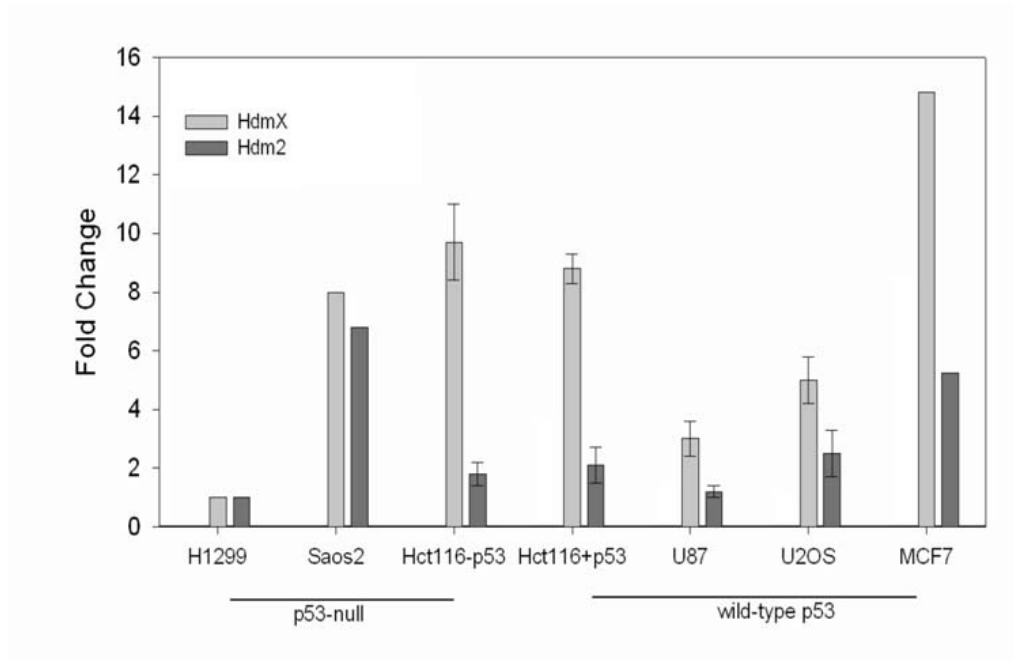
Given that HdmX and Hdm2 are overexpressed in approximately 17% of human tumors [16] the majority of which possess wild-type p53, this study set out to examine how loss of Hdm2/X affected gene expression and tumor cell growth. MCF7, which possess wild-type p53 [25] and elevated levels of both HdmX and Hdm2 (Figure 1A) was the tumor cell line used in these studies. To inactivate HdmX and Hdm2 we employed siRNA targeting each gene as described in the materials and methods.

Before performing the Affymetrix GeneChip experiments we developed a triple transfection protocol that led to over 90% of the MCF7 cells taking up the siRNA (data not shown). Next, the effectiveness of the knockdown was assessed using RT-qPCR (data not shown) and Western blotting. Following the triple transfection protocol HdmX and p53 protein levels were undetectable with Hdm2 showing a greater than 80% reduction in protein expression (Figure 1B). As expected, the loss of either HdmX or Hdm2 led to an increase in the levels of p21. This p21 increase is p53-dependent since no increase in p21 protein levels was detected upon concurrent knockdown of HdmX and p53. While it has been suggested that Hdm2 controls the levels of p53 in non-stressed cells [26, 27], in our hands MCF7 cells showed only a slight increase in p53 protein levels following the combined loss of HdmX and Hdm2. The inability of Hdm2 knockdown to result in an increase in p53 protein could be the result of MCF7 cells harboring an elevated level of HdmX. Consistent with this suggestion, the treatment of MCF7 cells with Nutlin leads to increased p53 protein levels through loss of Hdm2 binding to p53 and concurrent Hdm2 mediated degradation of HdmX [28].

Loss of Hdm2 and HdmX triggers inhibition of cell growth

Other groups have reported that in cells where wild-type p53 is kept in check by overexpression of HdmX or Hdm2, their inhibition can trigger alterations in cell growth [29] and in some conditions apoptosis [30]. To assess the growth properties of RNAi knockdown of p53 regulators Hdm2 and HdmX, siRNA-transfected MCF7 cells were plated at low density in 6 well plates and allowed to grow for an additional 10 days. While transfection of siCon or sip53 resulted in only minimal changes in cell growth (Figure 2B), knockdown of either

A



B

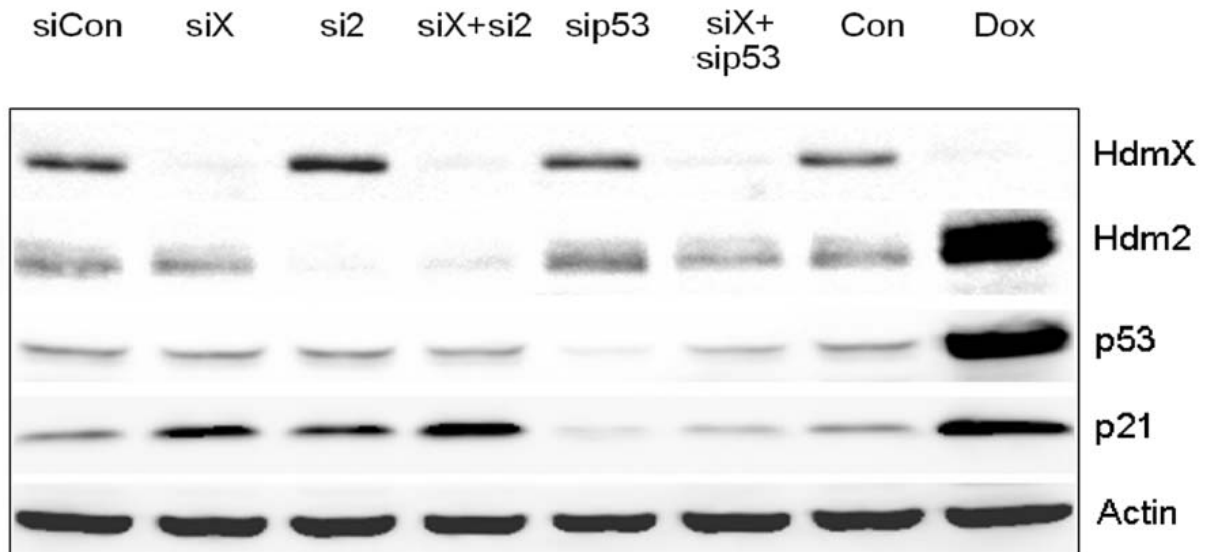


Figure 1. (A) RT-PCR analysis of *hdmX* and *hdm2* gene expression in various human cell lines. The endogenous levels of *hdmX* and *hdm2* were determined relative to H1299 cells. All samples were normalized to GAPDH. (B) RNAi knockdown of HdmX or Hdm2 triggers p53-dependent p21 induction. Western blot analysis of indicated proteins from the various siRNA or doxorubicin (Dox) treated MCF7 cells. Knockdowns of the indicated proteins were greater than 80%. Protein extracts were made 24 hours after the last siRNA transfection or treatment with 5 μ g/ml doxorubicin.

HdmX or Hdm2, alone or in combination led to significantly fewer colonies (Figure 2A) and suppressed cell growth when compared to siCon (Figure 2B). This

decrease in colony formation correlated with an increase in G1 arrest and not apoptosis (i.e. sub-G1) as determined by flow cytometry (data not shown).

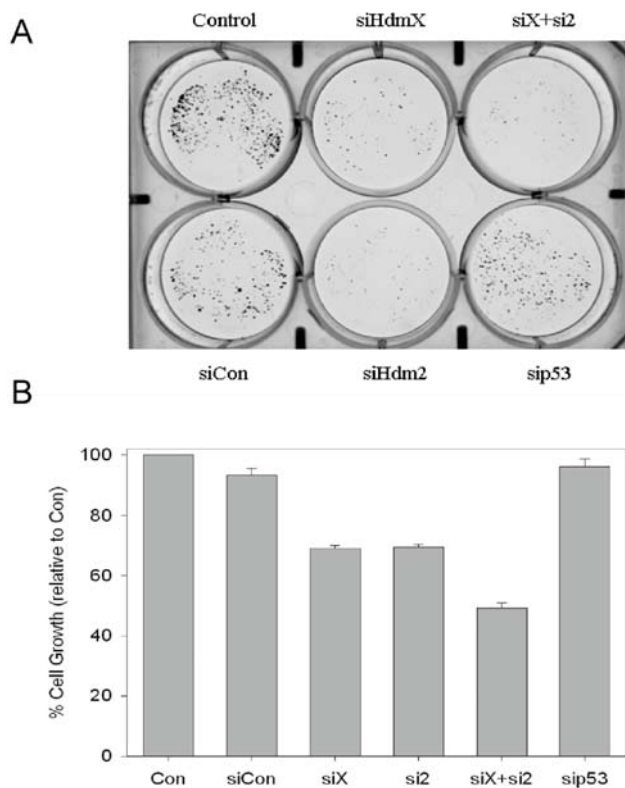


Figure 2. Loss of HdmX and/or Hdm2 inhibits MCF7 colony formation. (A) Following siRNA transfections, MCF7 cells were seeded at 500 cells/well in 6-well plates. The cells were allowed to grow for ten days then the colonies were stained with crystal violet. Significantly fewer colonies were present following knockdown of HdmX and/or Hdm2. The cells transfected with sip53 or a non-targeting control (siCon) showed minimal effects on colony formation relative to non-transfected control (Con/Control). (B) The percent cell growth relative to untransfected control was determined by extracting the stain in 10% acetic acid and quantifying the stain by reading absorbance at 590 nm.

Loss of HdmX or Hdm2 sensitizes MCF7 cells to DNA damage

Several recent studies using Nutlin and various DNA damaging agents reported that blocking Mdm2:p53 association led to increased chemosensitivity to DNA damaging agents [31, 32]. To examine whether knockdown of HdmX and Hdm2 can also elicit increased cytotoxicity to DNA damage, MCF7 cells were transfected with the indicated siRNA leading to alterations of gene expression (Figure 3B). Cells were then treated with varying doses of doxorubicin and cell viability assessed. siRNAs targeting HdmX or Hdm2 increased doxorubicin cytotoxicity, while removing

both HdmX and Hdm2 led to the greatest level of chemosensitivity (Figure 3A). Enhanced chemosensitivity was also observed in cisplatin treatment of siHdmX or siHdm2 MCF7 cells (data not shown).

Gene expression profiles of MCF7 cells lacking HdmX or Hdm2

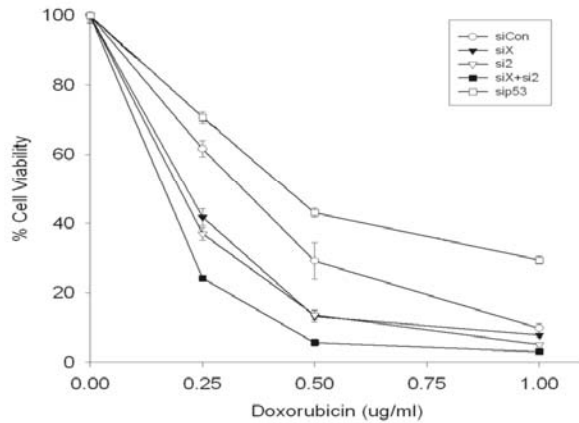
Having established an effective knockdown approach with effects on cell growth and increased sensitivity to DNA damage, we performed an Affymetrix GeneChip experiment to assess how loss of HdmX or Hdm2 affected global gene expression in MCF7 cells. Each RNAi transfection was performed in three separate biological replicates. The data analysis was carried out using GeneSpring GX software. Given the similarity of biological function uncovered in the previous experiments we focused our informatics on genes commonly altered following RNAi treatment with siHdmX or siHdm2. In summary, .cel files were normalized using GCRMA, genes filtered by ANOVA and fold change, and genes significantly altered by both siHdmX and siHdm2 but not siHdmX + sip53 identified (see materials and methods for detailed approach). From this approach we uncovered 394 gene alterations common to knockdown of both siHdmX and siHdm2 (Table 1).

p53 activation following loss of HdmX or Hdm2 triggers growth repressive genes

The initial examination of the 394 genes focused on those genes (n=222) that were increased following siHdmX or siHdm2 treatment relative to siCon. Thirteen genes were identified that were known p53-regulated genes (Figure 4). As expected these genes increased with siHdmX or siHdm2 treatment but had expression levels comparable or lower than siCon when treated with siHdmX+sip53 or sip53. Interestingly, with the exception of Fas, this list of p53 target genes consisted predominately of genes encoding proteins involved in cell cycle arrest or DNA repair. Consistent with a model whereby p53 proapoptotic target genes require p53 that is phosphorylated at serine 46 by HIPK2 [33-35], we observed no detectable phosphorylation at serines 6, 15, 20, 46, or 392 following the RNAi transfection protocol employed in these studies (data not shown).

To confirm these results, we performed RT-qPCR using TaqMan primers targeting five known p53 target genes, three of which were identified in our analysis. p21, BTG2 and ACTA2 are p53 target genes that are associated with cell cycle arrest or growth inhibition [36-38], while Hdm2 is a negative regulator of p53 and Noxa a pro-apoptotic factor not observed in our list of

A



B

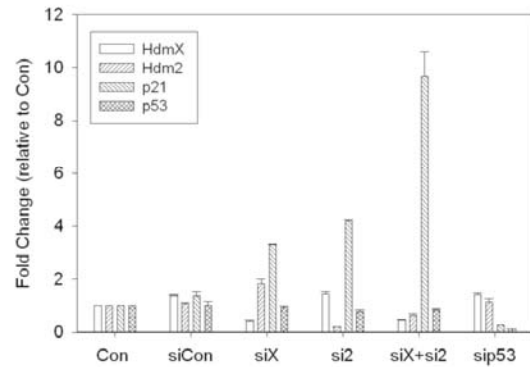


Figure 3. Knockdown of HdmX enhances doxorubicin-induced cytotoxicity. (A) Percent cell viability relative to untransfected untreated control cells. MCF7 cells were treated with doxorubicin (0.25-1.0 $\mu\text{g}/\text{mL}$) for 48 hours and cell viability was determined by absorbance at 590 nm. The loss of HdmX and/or Hdm2 showed an enhanced cytotoxicity relative to control cells. (B) RT-qPCR analysis of hdmX, hdm2, p21 and p53 gene expression in the indicated siRNA transfected MCF7 cells. The hdmX, hdm2, and p53 transcripts were effectively knocked down by siRNA prior to drug treatment.

altered genes [39]. MCF7 cells were either mock transfected (Mock), transfected with siRNA that does not target any human gene (siCon) or transfected with siRNA to HdmX or Hdm2 either alone or in combination. The results in Figure 5 demonstrate that relative to siCon, knockdown of HdmX led to significant increases in hdm2, p21, BTG2 and ACTA2 gene expression. No significant change in gene expression was observed with Noxa, which is consistent with our GeneChip results. With the obvious exception of hdm2, siRNA-targeting Hdm2 led to similar alterations in gene expression (Figure 5). Finally, when both HdmX and Hdm2 were eliminated, the levels of the cell cycle arrest genes p21, BTG2 and ACTA2 increased either synergistically or additively while levels of Noxa remained unchanged. These results validate our GeneChip data that p53-target genes were induced upon HdmX or Hdm2 knockdown and that several of these genes encode proteins involved in the cell cycle arrest.

p53 upregulation of p21 leads to global repression of E2F regulated genes

After searching for genes that were directly upregulated by p53 we next evaluated those genes that were repressed (N=172) following HdmX and Hdm2 knockdown (Figure 7). Within the list of downregulated genes were a set of genes that encode proteins involved in G1-S phase transition, the majority of which were known E2F1 regulated genes. It is

concomitant decrease in both CCNA2 and E2F1 (Figure 7). In contrast, loss of Hdm2/X and p21 completely abrogated CCNA2 and E2F1 repression consistent with p53 activation inactivating E2F1 transactivation via p21 induction.

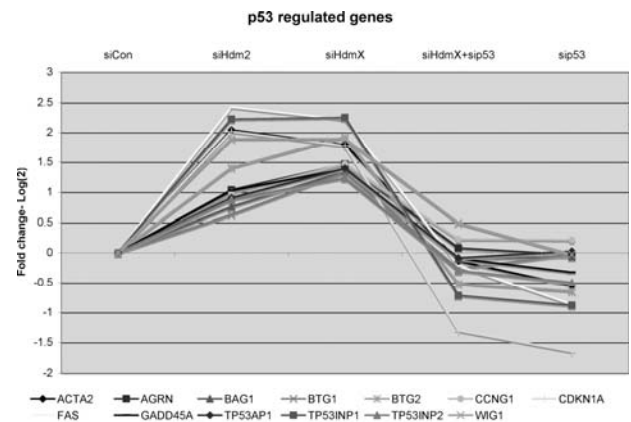


Figure 4. GeneChip expression of 13 known p53-regulated genes that were induced by knockdown of either siHdmX or siHdm2. Y-axis represents the average fold change (\log_2) for each of the genes in the indicated siRNA transfections relative to siCon (X-axis, conditions labeled at the top of the chart).

DISCUSSION

As an essential tumor suppressor it is no surprise that human tumors demonstrate a diverse array of genetic mechanisms to inactivate p53 function. Central to this present study are tumors where one or both of the negative regulators of p53, Hdm2 and HdmX, are overexpressed leading to loss of p53 activity. Previous studies have focused on Hdm2 overexpression, where a small molecule inhibitor Nutlin 3 has proven to activate wild-type p53 in cell lines with elevated Hdm2, triggering apoptosis when combined with genotoxic agents that do not function as anti-mitotics [44]. Unfortunately, Nutlins have not proven as effective in tumors where HdmX is overexpressed [18, 45-47], suggesting the need for additional approaches aimed at blocking the HdmX:p53 association particularly given the recent observation of HdmX overexpression in retinoblastoma [48].

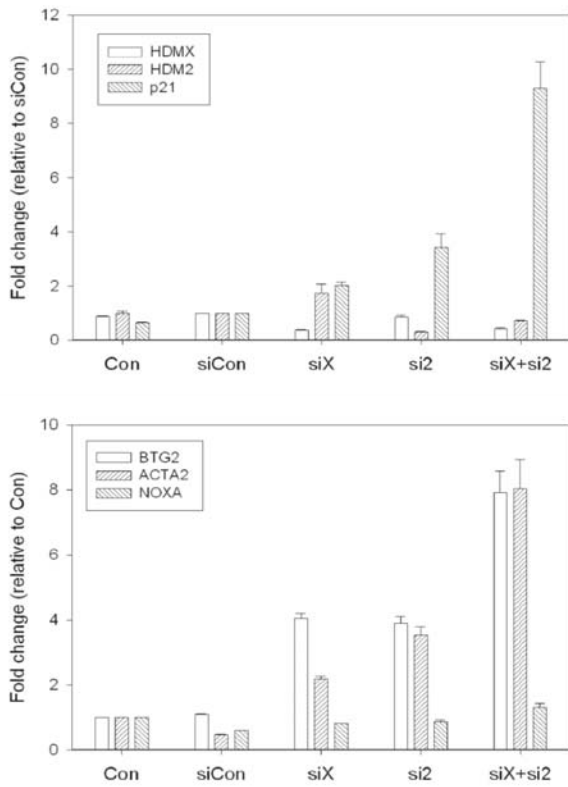


Figure 5. RT-qPCR validation of siRNA knockdown in MCF7 cells. (A) The hdmX, hdm2, and p21 mRNA expression relative to siCon (non-targeting siRNA) is shown. The p21 transcript is induced following loss of HdmX or Hdm2, and synergistically induced following loss of both HdmX and Hdm2. (B) BTG2, ACTA2, and NOXA mRNA expression relative to untransfected control (Con). The p53 target genes, BTG2 and ACTA2, are induced by loss of HdmX and/or Hdm2, while the expression of the proapoptotic gene, NOXA, is not altered.

Here we have employed RNAi approaches and DNA microarrays to better understand the activation of p53 in cells overexpressing Hdm2 and HdmX. In MCF7 cells a growth arrest with no detectable apoptosis was observed following knockdown of either Hdm2 or HdmX (Figure 2 and data not shown). While loss of either HdmX or Hdm2 was sufficient to trigger an anti-proliferative effect, the combined loss of both HdmX and Hdm2 resulted in a more significant growth inhibition.

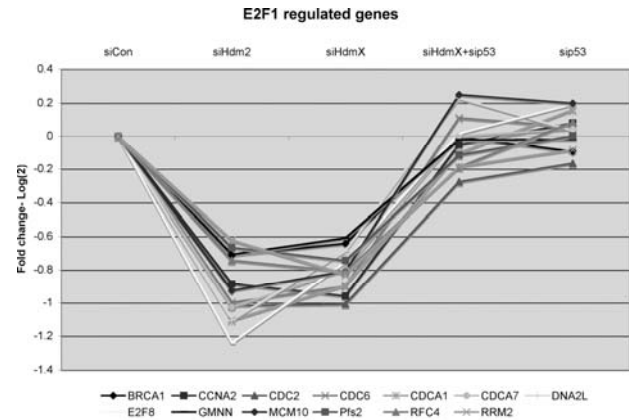


Figure 6. GeneChip expression of 13 reported E2F1-regulated genes that were repressed by knockdown of either siHdmX or siHdm2. Y-axis represents the average fold change (\log_2) for each of the genes in the indicated siRNA transfections relative to siCon (X-axis, conditions labeled at the top of the chart).

Even though this RNAi approach appears to activate p53 without triggering its phosphorylation (data not shown), the loss of either HdmX or Hdm2 did effectively sensitize the cells to doxorubicin with the loss of both Hdm2 and HdmX being most sensitive to DNA damage (Figure 3). Surprisingly our results showed only a modest elevation of endogenous p53 levels following loss of HdmX and Hdm2 (Figure 1). This result maybe unique to MCF7 cells which harbor elevated Hdm2 and HdmX, in contrast to most tumor cell lines with wild-type p53 that possessed only elevated Hdm2 (Figure 1A). Consistent with the need for only one negative regulator to be elevated 65% of retinoblastoma tumors overexpress HdmX and possess wild-type p53 [48]. Based on our previous HdmX overexpression studies [10] we would predict that the overexpression of HdmX might inhibit Hdm2 degradation of p53 in MCF7 cells and thus could explain why modulating Hdm2 levels in MCF7 cells has no dramatic effect on p53 levels.

The DNA microarray experiment directly tested whether HdmX or Hdm2 knockdown triggered an increase in p53-regulated genes. While 394 genes were

significantly altered by either HdmX or Hdm2 knockdown (Table 1), only a small group was previously identified p53 targets (Figure 4). A few of the remaining genes induced by HdmX or Hdm2 loss are likely novel p53 regulated genes (S. Berberich, personal communication) but most probably represent downstream effects of the cell cycle arrest induced by p53. Within the 13 identified p53 target genes it is noteworthy that only one apoptotic gene (Fas) was found activated by loss of either HdmX or Hdm2. Upon careful examination of 16 known p53 pro-apoptotic genes we found that several of them were repressed following p53 knockdown, suggesting that their failure to be induced by loss of HdmX or Hdm2 was not a cell-type specific phenotype. Rather, we propose that the non-genotoxic release of p53 from Hdm2 of HdmX results in a preferential activation of growth arrest target genes, like p21 (Figure 5). This model is consistent with recent work suggesting that p53 promoter selection is dependent on its phosphorylation [49].

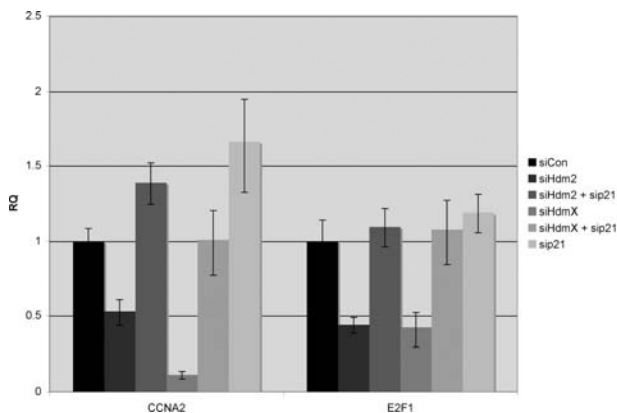


Figure 7. Repression of E2F1-regulated genes by Hdm2 or HdmX knockdown is blocked by concurrent knockdown of p21. MCF7 cells were transfected with the indicated siRNA combinations. Twenty-four hours later, RNA was isolated and subjected to RT-qPCR to quantify expression of CCNA2, p21 and E2F1 after normalization to GAPDH. Expression levels (Y-axis) were relative to siCon and reported as RQ values. Error bars represent the 95% confidence interval of the relative expression.

Another interesting finding within the microarray data was a subgroup of genes that were repressed upon HdmX and Hdm2 knockdown and could be classified as known E2F-regulated genes. Other groups have noted that p53 activation of p21 could lead to the repression of TERT [42] or Chk2 [41], known E2F-target genes, and another group recently reported similar findings using microarray assays [50].

While this report focused on genes commonly regulated by HdmX and Hdm2, it is worth mentioning that within genes uniquely regulated by either HdmX or Hdm2 we did not observe any additional p53 regulated genes (M. Markey, personal communication). The common biological effects of HdmX or Hdm2-loss and significant overlap of gene expression patterns are in contrast to recent *in vivo* studies where the knockout of Mdm2 or MdmX in adult mouse tissues lead to non-overlapping roles in regards to regulating p53 activity [51]. We believe these findings point to either differences in cell culture versus tissue studies or more likely represent a significant departure in the roles that Hdm2 and HdmX play when expressed at physiological levels compared to the elevated levels in tumor cells.

Finally these studies demonstrate that non-genotoxic activation of p53 by knockdown of its inhibitors Hdm2 and HdmX leads to the induction of genes involved in cell-cycle arrest, as well as repression of genes along the E2F/Rb pathway that promote cell cycle entry. These alterations in gene expression resulted in a decreased population of proliferative cells without necessarily increasing apoptosis. A non-genotoxic activation of p53 is one possible mechanism for the reduction in cellular proliferation observed during aging. This further underscores the critical importance of tumor suppressor activation in senescence and organismal aging.

MATERIALS AND METHODS

Cell lines, antibodies, siRNA and chemotherapeutic agents. The human breast tumor cell line MCF7 was grown in Dulbecco's modified Eagle medium (DMEM) supplemented with 10% bovine growth serum (BGS), and 10 µg/ml gentamicin unless otherwise indicated. HdmX polyclonal antibody (Bethyl Laboratories, Inc.), p21 polyclonal antibody C-19 (Santa Cruz Biotechnology, Inc.), p53 monoclonal antibody Ab-6 (Oncogene), Hdm2 monoclonal antibody SMP-14 (Santa Cruz Biotechnology, Inc.) and beta-actin monoclonal antibody (Sigma, Inc.) were used as indicated. A phosphorylation-specific p53 polyclonal antibody kit (Cell Signaling Technology, Inc.) was utilized per manufacturer's protocol. Horseradish peroxidase (HRP)-conjugated anti-mouse or anti-rabbit secondary antibodies (Promega) were used with Super Signal substrate (Pierce) for chemiluminescence detection of proteins. siGENOME duplex RNA targeting mRNA from hdmX, hdm2, or p53, and a non-targeting control siRNA were obtained from Dharmacon Research, Inc. and siRNA transfection was performed using Oligofectamine or Lipofectamine 2000 (Invitrogen) as described below. Doxorubicin hydro-

chloride (Tocris Bioscience) was prepared as a 5 mg/ml stock solution in water.

siRNA transfection. Cells were seeded at 200,000 cells per well in 6-well plates (for RNA isolation), or at 700,000 cells per 6-cm dish (for protein extraction) in antibiotic free DMEM containing 1% BGS in a small volume. Cells were reverse transfected with 100 nM siRNA (Dharmacon Research, Inc.) at time of seeding using Lipofectamine 2000 (Invitrogen). After a five hour incubation, the media was removed and cells were refed with DMEM containing 10% BGS. Twenty hours later, the cells were transfected again with 100 nM siRNA in a small volume of serum free media using Oligofectamine (Invitrogen). After a four-hour incubation, an equal volume of DMEM containing 20% BGS was added to each well or dish without removing the transfection mixture. Total RNA was isolated 24 hours post siRNA transfection and protein was extracted at 48 hours post siRNA unless otherwise indicated.

Analysis of Affymetrix GeneChips. The Affymetrix HG-U133 plus 2.0 GeneChips containing probe sets detecting over 54,000 transcripts were used in this study and each transfection condition was performed in triplicate. GeneChip cel files were imported into GeneSpring GX and preprocessed by GCRMA. Measurements less than 0.01 were then set to 0.01, and each chip was normalized to the 50th percentile of the measurements taken from that chip. Extra background correction was never applied. Each gene was normalized to the median of the measurements for that gene, and then to the median of that gene's expression in the siCon condition.

Initially all genes were filtered in GeneSpring GX first by Welch ANOVA to find expression changes based on siRNA treatment, using a p-value cut off of 0.05 and the Benjamini and Hochberg False Discovery Rate as a multiple testing correction. The cross-gene error model was active and based on replicates. From this list, genes were removed which varied between the mock and siCon treatments by 1.5 fold with a p-value < 0.05. Next, lists of genes with expression changes of 1.5 fold and a p-value < 0.05 were then made for siHdm2 versus siCon and siHdmX versus siCon. We then eliminated all but the union between these two lists. One gene that was repressed in the siHdm2 condition but upregulated in the siHdmX condition (encoding hypothetical protein MGC5370) was manually removed. Finally, genes that were not changed 1.5 fold with a p-value of <0.05 between the siHdmX and siHdmX + sip53 conditions were removed leaving a total of 394 selected genes.

Quantitative RT-pPCR. Cells were lysed directly in the culture dish and total RNA was isolated using the RNeasy kit (Qiagen) according to manufacturer's protocol. The RNA was quantified by spectrophotometer reading at 260 nm, and 1 µg RNA was reverse transcribed with random hexamers to create cDNA using the TaqMan Reverse transcription kit (Applied Biosystems). Quantitative PCR was performed in a 96-well micro titer plate format on an ABI Prism 7900HT sequence detection system using 1 µl cDNA, TaqMan Universal PCR master mix and Assay-on-Demand Gene Expression products (Applied Biosystems) specific for genes of interest. Each cDNA sample was analyzed in triplicate and fold change relative to control was calculated based on a PCR efficiency of two and normalized to GAPDH (endogenous control) RNA levels. Average fold change and standard deviation were obtained from 2-3 biological replicate samples per treatment assayed in triplicate.

Western blot analysis. Frozen cells were lysed in an aqueous extraction buffer composed of 120 mM NaCl, 50 mM Tris-HCl (pH 8.0), 5 mM EGTA, 1 mM EDTA, 5 mM NaPPi, 10 mM NaF, 30 mM para-nitrophenylphosphate, 1 mM Benzamidine, 0.1% NP-40 (Ipegal Ca-630), 0.2 mM PMSF, and 1% protease inhibitor cocktail (Sigma), and soluble protein was recovered by centrifugation. Protein concentration was determined using Bradford reagent (Bio-Rad), and proteins were resolved on a sodium dodecyl sulfate-10% polyacrylamide gel followed by transfer of proteins to a polyvinylidene difluoride membrane (Millipore) using a Transblot system (Bio-Rad). Immunoblotting was performed as previously described [52] using appropriate primary antibodies at 1:1000-1:10,000 dilution and secondary antibodies (goat anti-mouse or goat anti-rabbit HRP-conjugated, Promega) at 1:5000-1:10,000 dilution. Blots were exposed to chemiluminescent reagent (Pierce) and protein was visualized on a FUJIFILM LAS-3000 image reader.

Colony formation and cell viability assays. Twenty-four hours after the second siRNA transfection, the cells were trypsinized, counted and seeded at 500 cells per well in 6-well plates for the colony formation assay. The cells were allowed to grow for ten days, and then the colonies were fixed and stained in 1% crystal violet in 70% methanol. The cell viability assays were performed in 96-well plates using either CellQuant-Blue™ Reagent (BioAssay Systems) according to manufacturer's protocol or by staining the cells with crystal violet, extracting the stain in 10% acetic acid, and then reading absorbance at 590 nm. Again, cells were trypsinized after the second siRNA transfection, counted and seeded at 20,000 cells per well. Cell

viability was determined at various time points post-seeding or following treatment with chemotherapeutic agents for the times indicated.

ACKNOWLEDGEMENTS

This work was funded by the National Cancer Institute (CA66430 to SJB). The Biomedical Sciences Ph.D. program and NIH supported KAH. MM was supported by NIH and the Center for Genomics Research. DNA microarray facilities and bioinformatic programs were provided by the Center for Genomics Research.

CONFLICT OF INTERESTS STATEMENT

The authors of this manuscript have no conflict of interests to declare.

REFERENCES

- Hollstein M, Rice K, Greenblatt MS, Soussi T, Fuchs R, Sorlie T, Hovig E, Smith-Sorensen B, Montesano R, and Harris CC. Database of p53 gene somatic mutations in human tumors and cell lines. *Nucleic Acids Res.* 1994; 22:3551-3555.
- Kubbutat MH and Vousden KH. Keeping an old friend under control: regulation of p53 stability. *Mol Med Today.* 1998; 4:250-256.
- Vousden KH and Lu X. Live or let die: the cell's response to p53. *Nat Rev Cancer.* 2002; 2:594-604.
- Marine JC and Jochemsen AG. Mdmx and Mdm2: brothers in arms? *Cell Cycle.* 2004; 3:900-904.
- Oliner JD, Peitenol JA, Thiagalingam S, Gyuris J, Kinzler KW, and Vogelstein B. Oncoprotein MDM2 conceals the activation domain of tumour suppressor p53. *Nature.* 1993; 362:857-860.
- Haupt Y, Maya R, and Oren M. Mdm2 promotes the rapid degradation of p53. *Nature.* 1997; 387:296.
- Kubbutat MHG, Jones SN, and Vousden KH. Regulation of p53 stability by Mdm2. *Nature.* 1997; 387:299-303.
- Sharp DA, Kratowicz SA, Sank MJ, and George DL. Stabilization of the MDM2 Oncoprotein by Interaction with the Structurally Related MDMX Protein. *J Biol Chem.* 1999; 274:38189-38196.
- Tanimura S, Ohtsuka S, Mitsui K, Shirouzu K, Yoshimura A, and Ohtsubo M. MDM2 interacts with MDMX through their RING finger domains. *FEBS Lett.* 1999; 447:5-9.
- Jackson MW and Berberich SJ. MdmX protects p53 from Mdm2-mediated degradation. *Mol. Cell. Biol.* 2000; 20:1001-1007.
- Stad R, Little NA, Xirodimas DP, Frenk R, van der Eb AJ, Lane DP, Saville MK, and Jochemsen AG. Mdmx stabilizes p53 and Mdm2 via two distinct mechanisms. *EMBO Rep.* 2001; 2:1029-1034.
- Shvarts A, Steegenga W, van Laar RNT, Dekker P, Bazuine M, van Ham R, van der Houven van Oordt W, Hateboer G, van der Eb A, and Jochemsen A. MDMX: a novel p53-binding protein with some functional properties of MDM2. *The EMBO Journal.* 1996; 15:5349-5357.
- de Graaf P, Little NA, Ramos YF, Meulmeester E, Letteboer SJ, and Jochemsen AG. Hdmx protein stability is regulated by the ubiquitin ligase activity of Mdm2. *J Biol Chem.* 2003; 278:38315-38324.
- Kawai H, Wiederschain D, Kitao H, Stuart J, Tsai KK, and Yuan ZM. DNA damage-induced MDMX degradation is mediated by MDM2. *J Biol Chem.* 2003; 278:45946-45953.
- Pan Y and J. Chen J. MDM2 promotes ubiquitination and degradation of MDMX. *Mol Cell Biol.* 2003; 23:5113-5121.
- Toledo F and Wahl GM. Regulating the p53 pathway: in vitro hypotheses, in vivo veritas. *Nat Rev Cancer.* 2006; 6:909-923.
- Kojima K, Konopleva M, Samudio IJ, Shikami M, Cabreira-Hansen M, McQueen T, Ruvolo V, Tsao T, Zeng Z, Vassilev LT, Andreeff M. MDM2 antagonists induce p53-dependent apoptosis in AML: implications for leukemia therapy. *Blood.* 2005; 106:3150-3159.
- Patton JT, Mayo LD, Singhi AD, Gudkov AV, Stark GR, and Jackson MW. Levels of HdmX expression dictate the sensitivity of normal and transformed cells to Nutlin-3. *Cancer Res.* 2006; 66:3169-3176.
- Vassilev, LT. Small-Molecule Antagonists of p53-MDM2 Binding: Research Tools and Potential Therapeutics. *Cell Cycle.* 2004; 3:419-421.
- Chene P. Inhibiting the p53-MDM2 interaction: an important target for cancer therapy. *Nat Rev Cancer.* 2003; 3:102-109.
- Linares LK and Scheffner M. The ubiquitin-protein ligase activity of Hdm2 is inhibited by nucleic acids. *FEBS Lett.* 2003; 554:73-76.
- Yu Y, Sun P, Sun LC, Liu GY, Chen GH, Shang LH, Wu HB, Hu J, Li Y, Mao YL, Sui GJ, and Sun XW. Downregulation of MDM2 expression by RNAi inhibits LoVo human colorectal adenocarcinoma cells growth and the treatment of LoVo cells with mdm2siRNA3 enhances the sensitivity to cisplatin. *Biochem Biophys Res Commun.* 2006; 339:71-78.
- Zhang R, Wang H, and Agrawal S. Novel antisense anti-MDM2 mixed-backbone oligonucleotides: proof of principle, in vitro and in vivo activities, and mechanisms. *Curr Cancer Drug Targets.* 2005; 5:43-49.
- Hu B, Gilkes DM, and Chen J. Efficient p53 activation and apoptosis by simultaneous disruption of binding to MDM2 and MDMX. *Cancer Res.* 2007; 67:8810-8817.
- Ramos YF, Stad R, Attema J, Peltenburg LT, van der Eb AJ, and Jochemsen AG. Aberrant expression of HDMX proteins in tumor cells correlates with wild-type p53. *Cancer Res.* 2001; 61:1839-1842.
- Fuchs SY, Adler V, Buschmann T, Wu X, and Ronai Z. Mdm2 association with p53 targets its ubiquitination. *Oncogene.* 1998; 17:2543-2547.
- Little NA and Jochemsen AG. Hdmx and Mdm2 can repress transcription activation by p53 but not by p63. *Oncogene.* 2001; 20:4576-4580.
- Xia M, Knezevic D, Tovar C, Huang B, Heimbrook DC, and Vassilev LT. Elevated MDM2 boosts the apoptotic activity of p53-MDM2 binding inhibitors by facilitating MDMX degradation. *Cell Cycle.* 2008; 7:1604-1612.
- Efeyan A, Ortega-Molina A, Velasco-Miguel S, Herranz D, Vassilev LT, and Serrano M. Induction of p53-dependent senescence by the MDM2 antagonist nutlin-3a in mouse cells of fibroblast origin. *Cancer Res.* 2007; 67:7350-7357.
- Vassilev LT, Vu BT, Graves B, Carvajal D, Podlaski F, Filipovic Z, Kong N, Kammlott U, Lukacs C, Klein C, Fotouhi N, and Liu EA.

In vivo activation of the p53 pathway by small-molecule antagonists of MDM2. *Science*. 2004; 303:844-848.

31. Barbieri E, Mehta P, Chen Z, Zhang L, Slack A, Berg S, and Shohet JM. MDM2 inhibition sensitizes neuroblastoma to chemotherapy-induced apoptotic cell death. *Mol Cancer Ther*. 2006; 5:2358-2365.

32. Coll-Mulet L, Iglesias-Serret D, Santidrian AF, Cosialls AM, de Frias M, Castano E, Campas C, Barragan M, de Sevilla AF, Domingo A, Vassilev LT, Pons G, and Gil J. MDM2 antagonists activate p53 and synergize with genotoxic drugs in B-cell chronic lymphocytic leukemia cells. *Blood*. 2006; 107:4109-4114.

33. D'Orazi G, Cecchinelli B, Bruno T, Manni I, Higashimoto Y, Saito S, Gostissa M, Coen S, Marchetti A, Del Sal G, Piaggio G, Fanciulli M, Appella E, and Soddu S. Homeodomain-interacting protein kinase-2 phosphorylates p53 at Ser 46 and mediates apoptosis. *Nat Cell Biol*. 2002; 4:11-19.

34. Hofmann TG, Moller A, Sirma H, Zentgraf H, Taya Y, Droge W, Will H, and Schmitz ML. Regulation of p53 activity by its interaction with homeodomain-interacting protein kinase-2. *Nat Cell Biol*. 2002; 4:1-10.

35. Oda K, Arakawa H, Tanaka T, Matsuda K, Tanikawa C, Mori T, Nishimori H, Tamai K, Tokino T, Nakamura Y, and Taya Y. p53AIP1, a potential mediator of p53-dependent apoptosis, and its regulation by Ser-46-phosphorylated p53. *Cell*. 2000; 102:849-862.

36. el-Deiry, WS. Regulation of p53 downstream genes [In Process Citation]. *Semin Cancer Biol*. 1998; 8:345-357.

37. Cui XS and Donehower LA. Differential gene expression in mouse mammary adenocarcinomas in the presence and absence of wild type p53. *Oncogene*. 2000; 19:5988-5996.

38. Boiko AD, Porteous S, Razorenova OV, Krivokrysenko VI, Williams BR, and Gudkov AV. A systematic search for downstream mediators of tumor suppressor function of p53 reveals a major role of BTG2 in suppression of Ras-induced transformation. *Genes Dev*. 2006; 20:236-252.

39. Oda E, Ohki R, Murasawa H, Nemoto J, Shibue T, Yamashita T, Tokino T, Taniguchi T, and Tanaka N. Noxa, a BH3-only member of the bcl-2 family and candidate mediator of p53-induced apoptosis [In Process Citation]. *Science*. 2000; 288:1053-1058.

40. Boulaire J, Fotedar A, and Fotedar R. The functions of the cdk-cyclin kinase inhibitor p21WAF1. *Pathol Biol (Paris)*. 2000; 48:190-202.

41. Gottifredi V, Karni-Schmidt O, Shieh SS, and Prives C. p53 down-regulates CHK1 through p21 and the retinoblastoma protein. *Mol Cell Biol*. 2001; 21:1066-1076.

42. Shats I, Milyavsky M, Tang X, Stambolsky P, Erez N, Brosh R, Kogan I, Braunstein I, Tzukerman M, Ginsberg D, and Rotter V. p53-dependent down-regulation of telomerase is mediated by p21waf1. *J Biol Chem*. 2004; 279:50976-50985.

43. Chen KY. Transcription factors and the down-regulation of G1/S boundary genes in human diploid fibroblasts during senescence. *Front Biosci*. 1997; 2:d417-426.

44. Carvajal D, Tovar C, Yang H, Vu BT, Heimbrook DC, and Vassilev LT. Activation of p53 by MDM2 antagonists can protect proliferating cells from mitotic inhibitors. *Cancer Res*. 2005; 65:1918-1924.

45. Hu B, Gilkes DM, Farooqi B, Sebt SM, and Chen J. MDMX overexpression prevents P53 activation by the MDM2 inhibitor nutlin. *J Biol Chem*. 2006.

46. Kranz D and Dobbstein M. Nongenotoxic p53 activation protects cells against S-phase-specific chemotherapy. *Cancer Res*. 2006; 66:10274-10280.

47. Wade M, Wong ET, Tang M, Vassilev LT and Wahl GM. Hdmx modulates the outcome of p53 activation in human tumor cells. *J Biol Chem*. 2006.

48. Laurie NA, SDonovan SL, Shih CS, Zhang J, Mills N, Fuller C, Teunisse A, Lam S, Ramos Y, Mohan A, Johnson D, Wilson M, et al. Inactivation of the p53 pathway in retinoblastoma. *Nature*. 2006; 444:61-66.

49. Mayo LD, Seo YR, Jackson MW, Smith ML, Rivera Guzman J, Korgaonkar CK, and Donner DB. Phosphorylation of human p53 at serine 46 determines promoter selection and whether apoptosis is attenuated or amplified. *J Biol Chem*. 2005; 280:25953-25959.

50. Scian MJ, Carchman EH, Mohanraj L, Stagliano KE, Anderson MA, Deb D, Crane BM, Kiyono T, Windle B, Deb SP, and Deb S. Wild-type p53 and p73 negatively regulate expression of proliferation related genes. *Oncogene*. 2008; 27:2583-2593.

51. Francoz S, Froment P, Bogaerts S, De Clercq S, Maetens M, Doumont G, Bellefroid E, and Marine JC. Mdm4 and Mdm2 cooperate to inhibit p53 activity in proliferating and quiescent cells in vivo. *Proc Natl Acad Sci U S A*. 2006; 103:3232-3237.

52. Berberich SJ, Litteral V, Mayo LD, Tabesh D, and Morris D. mdm-2 gene amplification in 3T3-L1 preadipocytes. *Differentiation*. 1999; 64:205-212.

Table 1: Genes deregulated by HdmX and Hdm2 in MCF7 cells.

AffyID	Fold Change vs. siCon		Gene	Description
	siHdmX	siHdm2	Symbol	
212354 at	5.673	2.914	SULF1	sulfatase 1
205916 at	5.6	2.427	S100A7	S100 calcium binding protein A7 (psoriasin 1)
211163 s at	5.167	6.472	TNFRSF10C	tumor necrosis factor receptor superfamily, member 10c, decoy without an intracellular domain
206222 at	4.986	7.782	TNFRSF10C	tumor necrosis factor receptor superfamily, member 10c, decoy without an intracellular domain
208180 s at	4.603	4.544	HIST1H4H	histone 1, H4h
206488 s at	4.424	3.301	CD36	CD36 antigen (collagen type I receptor, thrombospondin receptor)
237737 at	4.4	4.846	LOC375010	hypothetical LOC375010 ; hypothetical LOC401131
232035 at	4.209	4.263	HIST1H4H	histone 1, H4h
216252 x at	3.97	5.55	FAS	Fas (TNF receptor superfamily, member 6)
213110 s at	3.929	3.082	COL4A5	collagen, type IV, alpha 5 (Alport syndrome)
209555 s at	3.927	3.001	CD36	CD36 antigen (collagen type I receptor, thrombospondin receptor)
229331 at	3.756	4.49	SPATA18	spermatogenesis associated 18 homolog (rat)
228766 at	3.703	1.865	CD36	CD36 antigen (collagen type I receptor, thrombospondin receptor)
208083 s at	3.664	3.871	ITGB6	integrin, beta 6
212097 at	3.631	1.804	CAV1	caveolin 1, caveolae protein, 22kDa
204781 s at	3.627	5.375	FAS	Fas (TNF receptor superfamily, member 6)
202917 s at	3.61	1.752	S100A8	S100 calcium binding protein A8 (calgranulin A)
225912 at	3.59	4.665	TP53INP1	tumor protein p53 inducible nuclear protein 1
215856 at	3.493	2.626	CD33L3	CD33 antigen-like 3
215719 x at	3.479	5.572	FAS	Fas (TNF receptor superfamily, member 6)
226535 at	3.47	3.972	ITGB6	integrin, beta 6
212344 at	3.331	2.234	SULF1	sulfatase 1
202833 s at	3.198	1.717	SERPINA1	serpin peptidase inhibitor, clade A (alpha-1 antiproteinase, antitrypsin), member 1
209504 s at	3.138	3.235	PLEKHB1	pleckstrin homology domain containing, family B (evectins) member 1
218692 at	3.104	2.476	FLJ20366	hypothetical protein FLJ20366
208096 s at	3.103	1.783	COL21A1	collagen, type XXI, alpha 1 ; collagen, type XXI, alpha 1
204780 s at	3.049	4.444	FAS	Fas (TNF receptor superfamily, member 6)
208683 at	3.027	2.795	CAPN2	calpain 2, (m//l) large subunit
219628 at	2.982	3.714	WIG1	p53 target zinc finger protein
211429 s at	2.976	1.724	SERPINA1	serpin peptidase inhibitor, clade A (alpha-1 antiproteinase, antitrypsin), member 1
1554062 at	2.871	3.334	XG	Xg blood group (pseudoautosomal boundary-divided on the X chromosome)
207695 s at	2.847	1.969	IGSF1	immunoglobulin superfamily, member 1
212298 at	2.819	2.164	NRP1	neuropilin 1
201236 s at	2.8	2.654	BTG2	BTG family, member 2
207392 x at	2.795	1.882	UGT2B15	UDP glucuronosyltransferase 2 family, polypeptide B15
215125 s at	2.784	1.964	UGT1A10 ; U	UDP glucuronosyltransferase 1 family, polypeptide A10
210387 at	2.776	2.855	HIST1H2BG	histone 1, H2bg

Table 1: Genes deregulated by HdmX and Hdm2 in MCF7 cells.

AffyID	Fold Change vs. siCon		Gene	Description
	siHdmX	siHdm2	Symbol	
208596_s_at	2.739	2.215	UGT1A10 ; U	UDP glucuronosyltransferase 1 family, polypeptide A10
208084_at	2.687	3.504	ITGB6	integrin, beta 6
242444_at	2.665	2.379	C1QTNF6	C1q and tumor necrosis factor related protein 6
212998_x_at	2.65	2.139	HLA-DQB1	major histocompatibility complex, class II, DQ beta 1 ; major histocompatibility complex, class II, DQ beta 1
202743_at	2.648	2.41	PIK3R3	phosphoinositide-3-kinase, regulatory subunit 3 (p55, gamma)
202688_at	2.635	2.027	TNFSF10	tumor necrosis factor (ligand) superfamily, member 10 ; tumor necrosis factor (ligand) superfamily, member 10
205306_x_at	2.633	3.434	KMO	kynurenine 3-monooxygenase (kynurenine 3-hydroxylase)
212347_x_at	2.62	2.552	MXD4	MAX dimerization protein 4
211161_s_at	2.581	1.685	COL3A1	collagen, type III, alpha 1 (Ehlers-Danlos syndrome type IV, autosomal dominant)
227863_at	2.577	2.524	CTSD	cathepsin D (lysosomal aspartyl peptidase)
220999_s_at	2.573	3.036	CYFIP2	cytoplasmic FMR1 interacting protein 2 ; cytoplasmic FMR1 interacting protein 2
1559116_s_at	2.559	1.995	AD-020	Chromosome 1 open reading frame 119
222150_s_at	2.555	2.22	LOC54103	hypothetical protein LOC54103
206280_at	2.533	1.924	CDH18	cadherin 18, type 2
228315_at	2.528	3.249		CDNA FLJ31683 fis, clone NT2RI2005353
1557779_at	2.523	2.226		Homo sapiens, clone IMAGE:4400004, mRNA
200974_at	2.52	4.108	ACTA2	actin, alpha 2, smooth muscle, aorta
221756_at	2.511	2.171	MGC17330	HGFL gene ; HGFL gene
202180_s_at	2.505	2.634	MVP	major vault protein
221218_s_at	2.484	2.759	TPK1	thiamin pyrophosphokinase 1
219049_at	2.479	1.767	ChGn	chondroitin beta1,4 N-acetylgalactosaminyltransferase
227020_at	2.448	2.095	YPEL2	yippee-like 2 (Drosophila)
225207_at	2.441	2.274	PDK4	pyruvate dehydrogenase kinase, isoenzyme 4
215779_s_at	2.439	2.315	HIST1H2BG	histone 1, H2bg
210778_s_at	2.432	1.917	MXD4	MAX dimerization protein 4
202284_s_at	2.428	4.05	CDKN1A	cyclin-dependent kinase inhibitor 1A (p21, Cip1)
211580_s_at	2.405	1.801	PIK3R3	phosphoinositide-3-kinase, regulatory subunit 3 (p55, gamma)
213261_at	2.388	1.842	LBA1	lupus brain antigen 1
215785_s_at	2.388	3.311	CYFIP2	cytoplasmic FMR1 interacting protein 2
210218_s_at	2.381	2.055	SP100	nuclear antigen Sp100
215465_at	2.375	2.541	ABCA12	ATP-binding cassette, sub-family A (ABC1), member 12
203058_s_at	2.365	2.382	PAPSS2	3'-phosphoadenosine 5'-phosphosulfate synthase 2
200984_s_at	2.35	2.369	CD59	CD59 antigen p18-20 (antigen identified by monoclonal antibodies 16.3A5, EJ16, EJ30, EL32 and G344)
225613_at	2.346	2.243	MAST4	microtubule associated serine/threonine kinase family member 4

Table 1: Genes deregulated by HdmX and Hdm2 in MCF7 cells.

AffyID	Fold Change vs. siHdmX	siCon siHdm2	Gene Symbol	Description
212463_at	2.34	2.5	CD59	CD59 antigen p18-20 (antigen identified by monoclonal antibodies 16.3A5, EJ16, EJ30, EL32 and G344)
204846_at	2.338	2.398	CP	ceruloplasmin (ferroxidase)
236835_at	2.336	1.973	FUT8	fucosyltransferase 8 (alpha (1,6) fucosyltransferase)
236278_at	2.333	2.228		
214616_at	2.322	2.008	HIST1H3E	histone 1, H3e
209737_at	2.31	2.216	MAGI2	membrane associated guanylate kinase, WW and PDZ domain containing 2
203060_s_at	2.304	2.3	PAPSS2	3'-phosphoadenosine 5'-phosphosulfate synthase 2
1552632_a_at	2.303	1.894	KIAA1001	Arylsulfatase G
209460_at	2.302	2.261	ABAT	4-aminobutyrate aminotransferase
207664_at	2.264	1.981	ADAM2	ADAM metalloproteinase domain 2 (fertilin beta)
200696_s_at	2.249	2.239	GSN	gelsolin (amyloidosis, Finnish type)
238439_at	2.24	2.4	ANKRD22	ankyrin repeat domain 22
223315_at	2.237	2.067	NTN4	netrin 4
224847_at	2.237	2.597	CDK6	cyclin-dependent kinase 6
242093_at	2.234	1.698		
223686_at	2.208	3.069	TPK1	thiamin pyrophosphokinase 1
210484_s_at	2.204	3.38	TNFRSF10C	tumor necrosis factor receptor superfamily, member 10c, decoy without an intracellular domain ; hypothetical protein MGC31957
201852_x_at	2.203	1.924	COL3A1	collagen, type III, alpha 1 (Ehlers-Danlos syndrome type IV, autosomal dominant)
1564573_at	2.193	2.13	LOC402778	similar to RIKEN cDNA 6330512M04 gene (mouse)
213744_at	2.192	1.528	ATRNL1	attractin-like 1
229553_at	2.192	1.863	PGM2L1	phosphoglucomutase 2-like 1
223600_s_at	2.191	2.291	KIAA1683	KIAA1683
209160_at	2.185	2.108	AKR1C3	aldo-keto reductase family 1, member C3 (3-alpha hydroxysteroid dehydrogenase, type II)
211138_s_at	2.18	2.362	KMO	kynurenine 3-monooxygenase (kynurenine 3-hydroxylase)
228390_at	2.179	1.883		CDNA clone IMAGE:5259272
206463_s_at	2.172	2.849	DHRS2	dehydrogenase/reductase (SDR family) member 2
212346_s_at	2.169	2.327	MXD4	MAX dimerization protein 4
1555756_a_at	2.164	1.907	CLEC7A	C-type lectin domain family 7, member A
214455_at	2.15	1.773	HIST1H2BC	histone 1, H2bc
228151_at	2.148	1.989		Transcribed locus
1559322_at	2.145	2.587	PTP4A1	Protein tyrosine phosphatase type IVA, member 1
203543_s_at	2.127	1.708	KLF9	Kruppel-like factor 9
205776_at	2.124	1.96	FMO5	flavin containing monooxygenase 5
206110_at	2.122	2.096	HIST1H3H	histone 1, H3h
40016_g_at	2.119	2.19	MAST4	microtubule associated serine/threonine kinase family member 4
205059_s_at	2.114	2.441	IDUA	iduronidase, alpha-L-
202963_at	2.113	2.189	RFX5	regulatory factor X, 5 (influences HLA class II expression)
213664_at	2.105	2.326	SLC1A1	solute carrier family 1 (neuronal/epithelial high affinity glutamate transporter, system Xag), member 1
218280_x_at	2.101	2.187	HIST2H2AA	histone 2, H2aa

Table 1: Genes deregulated by HdmX and Hdm2 in MCF7 cells.

AffyID	Fold Change vs. siCon		Gene Symbol	Description
	siHdmX	siHdm2		
214696 at	2.1	2.282	MGC14376	hypothetical protein MGC14376
225725 at	2.091	2.788		CDNA FLJ31683 fis, clone NT2RI2005353
224848 at	2.075	2.117	CDK6	cyclin-dependent kinase 6
202964 s at	2.071	2.222	RFX5	regulatory factor X, 5 (influences HLA class II expression)
238935 at	2.07	2.278	RPS27L	Ribosomal protein S27-like
1568629 s at	2.055	2.066	PIK3R2	phosphoinositide-3-kinase, regulatory subunit 2 (p85 beta)
223201 s at	2.055	1.808	RP13-360B21	hypothetical protein FLJ22679
218346 s at	2.037	2.688	SESN1	sestrin 1
202291 s at	2.026	1.539	MGP	matrix Gla protein
203887 s at	2.013	1.968	THBD	thrombomodulin
230093 at	2.008	1.981	TSGA2	testis specific A2 homolog (mouse)
219099 at	2.002	2.401	C12orf5	chromosome 12 open reading frame 5
229441 at	1.996	1.589	PRSS23	Protease, serine, 23
215076 s at	1.988	1.606	COL3A1	collagen, type III, alpha 1 (Ehlers-Danlos syndrome type IV, autosomal dominant)
202073 at	1.973	2.071	OPTN	optineurin
202357 s at	1.968	1.822	BF	B-factor, properdin
227221 at	1.966	3		CDNA FLJ31683 fis, clone NT2RI2005353
205110 s at	1.957	1.806	FGF13	fibroblast growth factor 13
203888 at	1.953	1.979	THBD	thrombomodulin
203571 s at	1.941	1.905	C10orf116	chromosome 10 open reading frame 116
223878 at	1.935	1.539	INPP4B	inositol polyphosphate-4-phosphatase, type II, 105kDa
223179 at	1.934	2.243	YPEL3	yippee-like 3 (Drosophila)
205174 s at	1.916	1.606	QPCT	glutaminy-peptide cyclotransferase (glutaminy cyclase)
218113 at	1.908	1.569	TMEM2	transmembrane protein 2
235534 at	1.908	2.274		Homo sapiens, clone IMAGE:5723825, mRNA
200983 x at	1.903	2.087	CD59	CD59 antigen p18-20 (antigen identified by monoclonal antibodies 16.3A5, EJ16, EJ30, EL32 and G344)
211864 s at	1.885	2.053	FER1L3	fer-1-like 3, myoferlin (C. elegans)
206482 at	1.884	1.66	PTK6	PTK6 protein tyrosine kinase 6
223434 at	1.883	1.588	GBP3	guanylate binding protein 3
223196 s at	1.877	2.476	SESN2	sestrin 2
1553033 at	1.868	1.821	SYTL5	synaptotagmin-like 5
226771 at	1.856	2.23	ATP8B2	ATPase, Class I, type 8B, member 2
201798 s at	1.855	1.889	FER1L3	fer-1-like 3, myoferlin (C. elegans)
227134 at	1.854	2.659	SYTL1	synaptotagmin-like 1
202708 s at	1.846	1.881	HIST2H2BE	histone 2, H2be
229566 at	1.845	1.815	LOC440449	hypothetical gene supported by AF086204
205326 at	1.823	1.651	RAMP3	receptor (calcitonin) activity modifying protein 3
238673 at	1.82	1.691		Transcribed locus
222450 at	1.818	1.724	TMEPAI	transmembrane, prostate androgen induced RNA
225927 at	1.81	1.514	MAP3K1	mitogen-activated protein kinase kinase kinase 1
213142 x at	1.804	1.742	LOC54103	hypothetical protein LOC54103
1556308 at	1.803	2.048	FLJ33674	hypothetical protein FLJ33674
225822 at	1.803	2.181	MGC17299	hypothetical protein MGC17299
208796 s at	1.8	1.994	CCNG1	cyclin G1

Table 1: Genes deregulated by HdmX and Hdm2 in MCF7 cells.

AffyID	Fold Change vs. siCon		Gene	Description
	siHdmX	siHdm2	Symbol	
226403 at	1.795	1.785	TMC4	transmembrane channel-like 4
209333 at	1.794	1.599	ULK1	unc-51-like kinase 1 (C. elegans)
226864 at	1.794	1.541	PKIA	Protein kinase (cAMP-dependent, catalytic) inhibitor alpha
203059 s at	1.787	2.03	PAPSS2	3'-phosphoadenosine 5'-phosphosulfate synthase 2
214290 s at	1.773	1.898	HIST2H2AA	histone 2, H2aa
205726 at	1.766	1.86	DIAPH2	diaphanous homolog 2 (Drosophila)
219410 at	1.753	1.508	TMEM45A	transmembrane protein 45A
37996 s at	1.752	1.871	DMPK	dystrophia myotonica-protein kinase
200766 at	1.744	1.73	CTSD	cathepsin D (lysosomal aspartyl peptidase)
232306 at	1.742	1.779	CDH26	cadherin-like 26
217419 x at	1.732	1.94	AGRN	agrin
219561 at	1.723	1.849	COPZ2	coatamer protein complex, subunit zeta 2
216264 s at	1.718	1.998	LAMB2	laminin, beta 2 (laminin S)
212120 at	1.712	1.606	RHOQ	Ras homolog gene family, member Q
212285 s at	1.711	2.049	AGRN	agrin
218007 s at	1.707	1.645	RPS27L	ribosomal protein S27-like
230780 at	1.707	1.809		CDNA FLJ31839 fis, clone NT2RP7000086
207655 s at	1.7	2.051	BLNK	B-cell linker
231406 at	1.7	1.665	LOC401394	hypothetical LOC401394 ; hypothetical LOC402578
204462 s at	1.699	1.527	SLC16A2	solute carrier family 16 (monocarboxylic acid transporters), member 2
214481 at	1.699	1.542	HIST1H2AM	Histone 1, H2am
231766 s at	1.693	1.786	COL12A1	collagen, type XII, alpha 1
219687 at	1.692	1.503	HHAT	hedgehog acyltransferase
202376 at	1.69	1.527	SERPINA3	serpin peptidase inhibitor, clade A (alpha-1 antiproteinase, antitrypsin), member 3
204954 s at	1.689	2.736	DYRK1B	dual-specificity tyrosine-(Y)-phosphorylation regulated kinase 1B
208792 s at	1.677	1.825	CLU	clusterin (complement lysis inhibitor, SP-40,40, sulfated glycoprotein 2, testosterone-repressed prostate message 2, apolipoprotein J)
217529 at	1.676	1.979	LOC401394	hypothetical LOC401394 ; hypothetical LOC402578
218471 s at	1.673	1.821	BBS1	Bardet-Biedl syndrome 1
203767 s at	1.664	1.758	STS	steroid sulfatase (microsomal), arylsulfatase C, isozyme S
208791 at	1.663	2.024	CLU	clusterin (complement lysis inhibitor, SP-40,40, sulfated glycoprotein 2, testosterone-repressed prostate message 2, apolipoprotein J)
201648 at	1.654	1.684	JAK1	Janus kinase 1 (a protein tyrosine kinase)
209917 s at	1.646	1.874	TP53AP1	TP53 activated protein 1
212450 at	1.645	1.534	KIAA0256	KIAA0256 gene product
222043 at	1.636	1.867	CLU	clusterin (complement lysis inhibitor, SP-40,40, sulfated glycoprotein 2, testosterone-repressed prostate message 2, apolipoprotein J)
204546 at	1.625	2.033	KIAA0513	KIAA0513
236668 at	1.621	1.853		CDNA clone IMAGE:5312086
209623 at	1.618	1.859	MCCC2	methylcrotonoyl-Coenzyme A carboxylase 2 (beta)

Table 1: Genes deregulated by HdmX and Hdm2 in MCF7 cells.

AffyID	Fold Change vs. siHdmX	siCon siHdm2	Gene Symbol	Description
209360 s at	1.616	1.583	RUNX1	runt-related transcription factor 1 (acute myeloid leukemia 1; aml1 oncogene)
220613 s at	1.614	1.616	SYTL2	synaptotagmin-like 2
217767 at	1.613	1.596	C3	complement component 3
209166 s at	1.611	1.58	MAN2B1	mannosidase, alpha, class 2B, member 1
207813 s at	1.61	3.021	FDXR	ferredoxin reductase
217783 s at	1.609	1.626	YPEL5	yippee-like 5 (Drosophila)
201116 s at	1.608	1.764	CPE	carboxypeptidase E
209739 s at	1.6	1.817	PNPLA4	patatin-like phospholipase domain containing 4
219529 at	1.59	1.596	CLIC3	chloride intracellular channel 3
223195 s at	1.59	2.022	SESN2	sestrin 2
203725 at	1.589	2.034	GADD45A	growth arrest and DNA-damage-inducible, alpha
209216 at	1.583	1.712	WDR45	WD repeat domain 45
234644 x at	1.582	1.738		CDNA: FLJ22426 fis, clone HRC08780
214542 x at	1.581	1.637	HIST1H2AI	histone 1, H2ai
210886 x at	1.577	1.681	TP53AP1	TP53 activated protein 1
201939 at	1.575	1.54	PLK2	polo-like kinase 2 (Drosophila)
208890 s at	1.568	1.97	PLXNB2	plexin B2
211979 at	1.561	1.549	GPR107	G protein-coupled receptor 107
210241 s at	1.557	1.585	TP53AP1	TP53 activated protein 1
				v-erb-b2 erythroblastic leukemia viral oncogene homolog 2, neuro/glioblastoma derived oncogene homolog (avian)
210930 s at	1.557	1.629	ERBB2	ERBB2
218706 s at	1.557	1.533	NS3TP2	HCV NS3-transactivated protein 2
				BCL2-associated athanogene ; BCL2-associated athanogene
202387 at	1.545	1.691	BAG1	BAG1
225968 at	1.545	1.679	PRICKLE2	prickle-like 2 (Drosophila)
200920 s at	1.54	1.545	BTG1	B-cell translocation gene 1, anti-proliferative
216080 s at	1.539	1.537	FADS3	fatty acid desaturase 3
39248 at	1.537	1.845	AQP3	aquaporin 3
				dual-specificity tyrosine-(Y)-phosphorylation regulated kinase 1B
217270 s at	1.535	1.844	DYRK1B	DYRK1B
				selenium binding protein 1 ; selenium binding protein 1
214433 s at	1.534	1.634	SELENBP1	SELENBP1
210224 at	1.524	1.575	MR1	major histocompatibility complex, class I-related
224836 at	1.512	1.833	TP53INP2	tumor protein p53 inducible nuclear protein 2
212890 at	1.511	1.874	MGC15523	hypothetical protein MGC15523
214086 s at	0.666	0.605	PARP2	poly (ADP-ribose) polymerase family, member 2
213346 at	0.665	0.616	LOC93081	hypothetical protein BC015148
228559 at	0.665	0.657		CDNA clone IMAGE:6043059
227337 at	0.663	0.544	ANKRD37	ankyrin repeat domain 37
235425 at	0.663	0.554	SGOL2	shugoshin-like 2 (S. pombe)
204435 at	0.661	0.587	NUPL1	nucleoporin like 1
201890 at	0.66	0.636	RRM2	ribonucleotide reductase M2 polypeptide
220840 s at	0.66	0.588	C1orf112	chromosome 1 open reading frame 112
222843 at	0.658	0.543	FIGLN1	fidgetin-like 1
				SMC2 structural maintenance of chromosomes 2-like 1 (yeast)
204240 s at	0.657	0.631	SMC2L1	SMC2L1
228273 at	0.657	0.612	FLJ11029	Hypothetical protein FLJ11029
203625 x at	0.656	0.579	SKP2	S-phase kinase-associated protein 2 (p45)
218350 s at	0.656	0.613	GMNN	geminin, DNA replication inhibitor

Table 1: Genes deregulated by HdmX and Hdm2 in MCF7 cells.

AffyID	Fold Change vs. siHdmX	siCon siHdm2	Gene Symbol	Description
219502_at	0.656	0.492	NEIL3	nei endonuclease VIII-like 3 (E. coli)
209608_s_at	0.655	0.664	ACAT2	acetyl-Coenzyme A acetyltransferase 2 (acetoacetyl Coenzyme A thiolase)
203213_at	0.653	0.543	CDC2	Cell division cycle 2, G1 to S and G2 to M
227787_s_at	0.653	0.636	THRAP6	thyroid hormone receptor associated protein 6
219555_s_at	0.65	0.621	BM039	uncharacterized bone marrow protein BM039
203302_at	0.646	0.569	DCK	deoxycytidine kinase
222608_s_at	0.646	0.54	ANLN	anillin, actin binding protein (scraps homolog, Drosophila)
222740_at	0.646	0.473	ATAD2	ATPase family, AAA domain containing 2
216228_s_at	0.645	0.554	WDHD1	WD repeat and HMG-box DNA binding protein 1
222848_at	0.645	0.464	FKSG14	leucine zipper protein FKSG14
220865_s_at	0.644	0.641	TPRT	trans-prenyltransferase
205394_at	0.642	0.541	CHEK1	CHK1 checkpoint homolog (S. pombe)
223256_at	0.642	0.568	KIAA1333	KIAA1333
229442_at	0.642	0.618	C18orf54	chromosome 18 open reading frame 54
204531_s_at	0.641	0.61	BRCA1	breast cancer 1, early onset
209754_s_at	0.641	0.59	TMPO	thymopoietin
211767_at	0.641	0.613	SLD5	SLD5 homolog ; SLD5 homolog
223255_at	0.641	0.554	KIAA1333	KIAA1333
225300_at	0.641	0.639	C15orf23	chromosome 15 open reading frame 23
229886_at	0.641	0.627	FLJ32363	FLJ32363 protein
209709_s_at	0.638	0.638	HMMR	hyaluronan-mediated motility receptor (RHAMM)
218755_at	0.638	0.596	KIF20A	kinesin family member 20A
1568596_a_at	0.637	0.657	TROAP	trophinin associated protein (tastin)
219531_at	0.637	0.653	Cep72	centrosomal protein 72 kDa
227545_at	0.637	0.626	BARD1	BRCA1 associated RING domain 1
234944_s_at	0.637	0.597	FAM54A	family with sequence similarity 54, member A
238075_at	0.637	0.601	CHEK1	CHK1 checkpoint homolog (S. pombe)
204962_s_at	0.636	0.666	CENPA	centromere protein A, 17kDa
222039_at	0.636	0.582	LOC146909	hypothetical protein LOC146909
202705_at	0.635	0.651	CCNB2	cyclin B2
229610_at	0.635	0.603	FLJ40629	hypothetical protein FLJ40629
219650_at	0.634	0.605	FLJ20105	FLJ20105 protein
201663_s_at	0.633	0.618	SMC4L1	SMC4 structural maintenance of chromosomes 4-like 1 (yeast)
218883_s_at	0.633	0.641	MLF1IP	MLF1 interacting protein
209715_at	0.632	0.621	CBX5	chromobox homolog 5 (HP1 alpha homolog, Drosophila)
220239_at	0.629	0.626	KLHL7	kelch-like 7 (Drosophila)
209680_s_at	0.628	0.531	KIFC1	kinesin family member C1
218768_at	0.627	0.61	NUP107	nucleoporin 107kDa
38158_at	0.627	0.661	ESPL1	extra spindle poles like 1 (S. cerevisiae)
204127_at	0.626	0.6	RFC3	replication factor C (activator 1) 3, 38kDa
209714_s_at	0.625	0.629	CDKN3	cyclin-dependent kinase inhibitor 3 (CDK2-associated dual specificity phosphatase)
235545_at	0.625	0.556	DEPDC1	DEP domain containing 1
208955_at	0.624	0.604	DUT	dUTP pyrophosphatase
201896_s_at	0.623	0.65	PSRC1	proline/serine-rich coiled-coil 1
212621_at	0.622	0.623	KIAA0286	KIAA0286 protein
213647_at	0.622	0.465	DNA2L	DNA2 DNA replication helicase 2-like (yeast)

Table 1: Genes deregulated by HdmX and Hdm2 in MCF7 cells.

AffyID	Fold Change vs. siCon		Gene Symbol	Description
	siHdmX	siHdm2		
204822_at	0.62	0.523	TTK	TTK protein kinase
204825_at	0.62	0.606	MELK	maternal embryonic leucine zipper kinase
215773_x_at	0.62	0.664	PARP2	poly (ADP-ribose) polymerase family, member 2
204162_at	0.619	0.573	KNTC2	kinetochore associated 2
205393_s_at	0.619	0.561	CHEK1	CHK1 checkpoint homolog (S. pombe)
221685_s_at	0.619	0.555	FLJ20364	hypothetical protein FLJ20364
227928_at	0.619	0.523	FLJ20641	hypothetical protein FLJ20641
228069_at	0.619	0.575	FAM54A	family with sequence similarity 54, member A
230165_at	0.619	0.548	SGOL2	shugoshin-like 2 (S. pombe)
218585_s_at	0.618	0.555	DTL	denticleless homolog (Drosophila)
218355_at	0.616	0.638	KIF4A	kinesin family member 4A
223307_at	0.616	0.63	CDCA3	cell division cycle associated 3
218039_at	0.615	0.612	NUSAP1	nucleolar and spindle associated protein 1
204033_at	0.614	0.628	TRIP13	thyroid hormone receptor interactor 13
225687_at	0.613	0.621	C20orf129	chromosome 20 open reading frame 129
226308_at	0.61	0.633	NY-SAR-48	sarcoma antigen NY-SAR-48
204752_x_at	0.608	0.618	PARP2	poly (ADP-ribose) polymerase family, member 2
206653_at	0.608	0.473	POLR3G	Polymerase (RNA) III (DNA directed) polypeptide G (32kD)
210983_s_at	0.608	0.666	MCM7	MCM7 minichromosome maintenance deficient 7 (S. cerevisiae)
218782_s_at	0.608	0.5	ATAD2	ATPase family, AAA domain containing 2
219258_at	0.608	0.527	FLJ20516	timeless-interacting protein
208795_s_at	0.607	0.634	MCM7	MCM7 minichromosome maintenance deficient 7 (S. cerevisiae)
220060_s_at	0.607	0.506	FLJ20641	hypothetical protein FLJ20641
221436_s_at	0.607	0.623	CDCA3	cell division cycle associated 3 ; cell division cycle associated 3
223542_at	0.607	0.512	ANKRD32	ankyrin repeat domain 32
1553244_at	0.604	0.592	FANCB	Fanconi anemia, complementation group B
219004_s_at	0.604	0.627	C21orf45	chromosome 21 open reading frame 45
221591_s_at	0.603	0.647	FAM64A	family with sequence similarity 64, member A
203805_s_at	0.602	0.59	FANCA	Fanconi anemia, complementation group A ; Fanconi anemia, complementation group A
219978_s_at	0.601	0.579	NUSAP1	nucleolar and spindle associated protein 1
221879_at	0.601	0.596	CALML4	calmodulin-like 4
203755_at	0.6	0.577	BUB1B	BUB1 budding uninhibited by benzimidazoles 1 homolog beta (yeast)
203764_at	0.6	0.567	DLG7	discs, large homolog 7 (Drosophila)
204887_s_at	0.6	0.59	PLK4	polo-like kinase 4 (Drosophila)
206550_s_at	0.6	0.61	NUP155	nucleoporin 155kDa
227211_at	0.6	0.577	PHF19	PHD finger protein 19
205053_at	0.599	0.638	PRIM1	primase, polypeptide 1, 49kDa
64408_s_at	0.598	0.515	CALML4	calmodulin-like 4
221521_s_at	0.597	0.63	Pfs2	DNA replication complex GINS protein PSF2
222962_s_at	0.595	0.496	MCM10	MCM10 minichromosome maintenance deficient 10 (S. cerevisiae)
205519_at	0.594	0.533	WDR76	WD repeat domain 76
219990_at	0.594	0.423	E2F8	E2F transcription factor 8
213226_at	0.592	0.485	CCNA2	Cyclin A2
219703_at	0.592	0.44	MNS1	meiosis-specific nuclear structural 1

Table 1: Genes deregulated by HdmX and Hdm2 in MCF7 cells.

AffyID	Fold Change vs. siCon		Gene Symbol	Description
	siHdmX	siHdm2		
242584_at	0.589	0.516	FLJ13305	hypothetical protein FLJ13305
1552619_a_at	0.587	0.48	ANLN	anillin, actin binding protein (scraps homolog, Drosophila)
204603_at	0.583	0.503	EXO1	exonuclease 1
223570_at	0.583	0.502	MCM10	MCM10 minichromosome maintenance deficient 10 (S. cerevisiae)
204492_at	0.582	0.628	ARHGAP11A	Rho GTPase activating protein 11A
214240_at	0.582	0.643	GAL	galanin
219306_at	0.582	0.56	KIF15	kinesin family member 15
203145_at	0.581	0.645	SPAG5	sperm associated antigen 5
203968_s_at	0.581	0.561	CDC6	CDC6 cell division cycle 6 homolog (S. cerevisiae)
230847_at	0.58	0.521	WRNIP1	Werner helicase interacting protein 1
221520_s_at	0.578	0.662	CDCA8	cell division cycle associated 8
219294_at	0.577	0.509	C6orf139	chromosome 6 open reading frame 139
1552921_a_at	0.575	0.56	FIGNL1	fidgetin-like 1
224428_s_at	0.575	0.491	CDCA7	cell division cycle associated 7 ; cell division cycle associated 7
218663_at	0.573	0.579	HCAP-G	chromosome condensation protein G
1553984_s_at	0.572	0.643	DTYMK	deoxythymidylate kinase (thymidylate kinase)
220651_s_at	0.571	0.527	MCM10	MCM10 minichromosome maintenance deficient 10 (S. cerevisiae)
236641_at	0.571	0.48	KIF14	kinesin family member 14
204023_at	0.57	0.598	RFC4	replication factor C (activator 1) 4, 37kDa
205024_s_at	0.568	0.584	RAD51	RAD51 homolog (RecA homolog, E. coli) (S. cerevisiae)
218662_s_at	0.566	0.516	HCAP-G	chromosome condensation protein G
222958_s_at	0.566	0.473	DEPDC1	DEP domain containing 1
242787_at	0.565	0.526		
1554768_a_at	0.564	0.522	MAD2L1	MAD2 mitotic arrest deficient-like 1 (yeast)
204641_at	0.564	0.521	NEK2	NIMA (never in mitosis gene a)-related kinase 2
209773_s_at	0.564	0.65	RRM2	ribonucleotide reductase M2 polypeptide
223229_at	0.564	0.605	UBE2T	ubiquitin-conjugating enzyme E2T (putative)
201897_s_at	0.563	0.602	CKS1B	CDC28 protein kinase regulatory subunit 1B
214804_at	0.563	0.582	FSHPRH1	FSH primary response (LRPR1 homolog, rat) 1
225834_at	0.562	0.489	FAM72A	family with sequence similarity 72, member A
202954_at	0.56	0.641	UBE2C	ubiquitin-conjugating enzyme E2C
205909_at	0.557	0.55	POLE2	polymerase (DNA directed), epsilon 2 (p59 subunit)
205967_at	0.553	0.556	HIST1H4C	histone 1, H4c
212949_at	0.551	0.558	BRRN1	barren homolog (Drosophila)
1553528_a_at	0.548	0.438	TAF5	TAF5 RNA polymerase II, TATA box binding protein (TBP)-associated factor, 100kDa
207891_s_at	0.548	0.582	TREX2 ; UIP	three prime repair exonuclease 2 ; 26S proteasome-associated UCH interacting protein 1
219494_at	0.547	0.562	RAD54B	RAD54 homolog B (S. cerevisiae)
209891_at	0.546	0.504	SPBC25	spindle pole body component 25 homolog (S. cerevisiae)
205733_at	0.545	0.521	BLM	Bloom syndrome
227165_at	0.545	0.517	C13orf3	chromosome 13 open reading frame 3
210416_s_at	0.544	0.572	CHEK2	CHK2 checkpoint homolog (S. pombe)
215509_s_at	0.544	0.493	BUB1	BUB1 budding uninhibited by benzimidazoles 1 homolog (yeast)

Table 1: Genes deregulated by HdmX and Hdm2 in MCF7 cells.

AffyID	Fold Change vs. siCon		Gene Symbol	Description
	siHdmX	siHdm2		
37577_at	0.544	0.538	ARHGAP19	Rho GTPase activating protein 19
212619_at	0.542	0.501	KIAA0286	KIAA0286 protein
211080_s_at	0.541	0.524	NEK2	NIMA (never in mitosis gene a)-related kinase 2 ; NIMA (never in mitosis gene a)-related kinase 2
204128_s_at	0.54	0.562	RFC3	replication factor C (activator 1) 3, 38kDa
204126_s_at	0.539	0.606	CDC45L	CDC45 cell division cycle 45-like (S. cerevisiae)
223381_at	0.538	0.465	CDCA1	cell division cycle associated 1
203967_at	0.536	0.501	CDC6	CDC6 cell division cycle 6 homolog (S. cerevisiae)
220295_x_at	0.535	0.444	DEPDC1	DEP domain containing 1
242939_at	0.535	0.595	TFDP1	transcription factor Dp-1
222680_s_at	0.533	0.532	DTL	denticleless homolog (Drosophila)
232278_s_at	0.53	0.495	DEPDC1	DEP domain containing 1
204728_s_at	0.529	0.501	WDHD1	WD repeat and HMG-box DNA binding protein 1
210053_at	0.529	0.461	TAF5	TAF5 RNA polymerase II, TATA box binding protein (TBP)-associated factor, 100kDa
206632_s_at	0.522	0.526	APOBEC3B	apolipoprotein B mRNA editing enzyme, catalytic polypeptide-like 3B
202779_s_at	0.517	0.642	UBE2S	ubiquitin-conjugating enzyme E2S
209464_at	0.517	0.566	AURKB	aurora kinase B
203418_at	0.514	0.541	CCNA2	cyclin A2
223700_at	0.514	0.504	GAJ	GAJ protein
203214_x_at	0.507	0.505	CDC2	cell division cycle 2, G1 to S and G2 to M
218726_at	0.507	0.527	DKFZp762E1	hypothetical protein DKFZp762E1312
230021_at	0.501	0.575	MGC45866	leucine-rich repeat kinase 1
209408_at	0.498	0.564	KIF2C	kinesin family member 2C
211519_s_at	0.498	0.537	KIF2C	kinesin family member 2C
210559_s_at	0.497	0.494	CDC2	cell division cycle 2, G1 to S and G2 to M
219000_s_at	0.49	0.519	DCC1	defective in sister chromatid cohesion homolog 1 (S. cerevisiae)
239002_at	0.488	0.416	ASPM	asp (abnormal spindle)-like, microcephaly associated (Drosophila)
210334_x_at	0.483	0.544	BIRC5	baculoviral IAP repeat-containing 5 (survivin)

